
FEAT: A LINEAR-COMPLEXITY FOUNDATION MODEL FOR EXTREMELY LARGE STRUCTURED DATA

A PREPRINT

Zhenghang Song
Zhejiang University
22451060@zju.edu.cn

Tang Qian
Ant Group
qiantang.qt@antgroup.com

Lu Chen*
Zhejiang University
luchen@zju.edu.cn

Yushuai Li*
Aalborg University
yusli@cs.aau.dk

Zhengke Hu
Ant Group
zhengke.hzk@antgroup.com

Bingbing Fang
Ant Group
jianjiu.fbb@antgroup.com

Yumeng Song
Aalborg University
yumengs@cs.aau.dk

Junbo Zhao
Ant Group
zhaojunbo.zjb@antgroup.com

Sheng Zhang
Ant Group
sheng.zs@antgroup.com

Tianyi Li
Aalborg University
tianyi@cs.aau.dk

March 18, 2026

ABSTRACT

Structured data is widely used in domains such as healthcare, finance, e-commerce, and scientific data management. Large structured-data models (LDMs) extend the foundation model paradigm to this setting and enable unified modeling of heterogeneous structured datasets for tasks such as classification, regression, and decision support. However, existing LDMs still face major limitations on real-world datasets. First, most LDMs rely on sample-wise full self-attention, whose $\mathcal{O}(N^2)$ complexity severely limits the number of samples that can be processed. Second, directly replacing attention with linear sequence models often degrades representations on structured data due to hidden-state compression and artificial causal bias that conflicts with permutation-invariant samples. Third, synthetic-only pre-training often fails to match the heavy-tailed and heterogeneous distributions of real-world structured data. To address these limitations, we propose FEAT, a linear-complexity foundation model for extremely large structured data. FEAT introduces a multi-layer dual-axis encoding architecture that replaces quadratic attention with hybrid linear encoding. The architecture combines two linear-complexity encoding layers, adaptive-fusion bi-Mamba-2 (AFBM) for modeling local dependencies across samples and convolutional gated linear attention (Conv-GLA) for maintaining global memory. This design enables linear-complexity cross-sample modeling while preserving expressive representations for large-scale structured data. To improve robustness in pre-training, FEAT further adopts a hybrid structural causal model pipeline together with a stable reconstruction objective designed for heavy-tailed structured distributions. Experiments on 11 real-world structured-data datasets show that FEAT consistently outperforms several representative baselines in zero-shot performance, while scaling linearly with the number of samples, achieving up to 40× faster inference.

Keywords Large Structured-Data Models · Foundation Models · Linear Complexity · In-Context Learning

1 Introduction

Structured data refers to information organized according to a predefined data model or schema, typically instantiated as matrices where each record represents a sample and each dimension corresponds to a specific feature or attribute. It is widely used in many domains, including genomics, healthcare, finance, e-commerce, and scientific data management Hollmann et al. [2025], Borisov et al. [2024]. Analyzing structured data enables the discovery of

complex relational patterns, the prediction of future outcomes, and the support of automated decision-making. Such capabilities are critical in applications like disease diagnosis, risk assessment, algorithmic trading, and personalized recommendation systems.

Most predictive modeling methods for structured data Grinsztajn et al. [2022] rely on tree-based ensembles Breiman [2001], Chen and Guestrin [2016], Ke et al. [2017], Prokhorenkova et al. [2018] or specialized deep networks Arik and Pfister [2021], Gorishniy et al. [2021], Somepalli et al. [2021]. These approaches typically require task-specific training on each dataset, involving extensive hyperparameter tuning and large amounts of labeled data. Such requirements limit their ability to generalize across datasets and tasks.

Foundation models (FMs) Bommasani et al. [2021] provide an alternative paradigm. They are large-scale models trained on massive datasets and designed to generalize across tasks. This paradigm has significantly improved performance in natural language processing and computer vision Brown et al. [2020], Touvron et al. [2023], Dosovitskiy et al. [2021]. Extending FMs to structured data has therefore become an important research direction. Existing models, such as TabPFN Hollmann et al. [2025] and LimiX Han et al. [2025], typically employ Transformer Vaswani et al. [2017] pre-trained on large synthetic structured datasets. They formulate structured data prediction as an in-context learning (ICL) problem Qu et al. [2025], allowing models to perform few-shot inference without dataset-specific retraining.

While existing studies demonstrate promising performance on small-scale datasets, they still face three major challenges when deployed on real-world datasets:

Challenge I: How to reduce the quadratic complexity of cross-sample modeling for massive structured datasets? To capture the macroscopic distribution of structured data, LDMs rely on full self-attention for cross-sample modeling. However, the inherent quadratic complexity ($\mathcal{O}(N^2)$) of self-attention severely restricts the context window, consistently triggering kernel-error or out-of-memory failures near just 50,000 samples Qu et al. [2025], Ma et al. [2024], Grinsztajn et al. [2025]. While heuristic divide-and-conquer strategies can mitigate this at test time Ye et al. [2025], they cannot circumvent the fundamental computational bottleneck during pre-training. Since real-world structured datasets routinely exceed millions of records Thomas et al. [2024], this persistent $\mathcal{O}(N^2)$ barrier strictly prohibits standard LDMs from ever observing the true global data distribution.

Challenge II: How to maintain expressive representations under linear-complexity modeling on permutation-invariant structured data? To bypass the $\mathcal{O}(N^2)$ bottleneck, an intuitive approach is to adopt linear-complexity ($\mathcal{O}(N)$) sequence models, such as State Space Models (SSMs) Gu and Dao [2024] or Linear Attention Katharopoulos et al. [2020]. However, directly transplanting these architectures to structured data precipitously leads to representation collapse Ahamed and Cheng [2024], Koch et al. [2025]. The fundamental disconnect lies in the data topology: standard linear models are inherently designed for sequential data driven by temporal locality and sequential dependencies. Conversely, structured datasets are strictly permutation-invariant—the order of records carries no semantic meaning. When recurrent-like SSMs process unordered tabular samples, their fixed-size hidden states are forced to compress global, non-directional interactions into a rigid computational bottleneck. This inherently imposes a detrimental “recency bias” that arbitrarily prioritizes newly observed records while catastrophically forgetting earlier global context, severely degrading the model’s expressive capacity. Conversely, while Linear Attention mechanisms avoid strict state compression and better preserve global routing, they critically lack the aggressive dynamic filtering required to suppress the heavy intrinsic noise of structured features, allowing variance to destructively accumulate over massive contexts Yang et al. [2024]. Consequently, existing linear models are structurally inadequate.

Challenge III: How to ensure stable optimization under heavy-tailed real-world structured data? Most existing structured-data FMs pre-train on synthetic datasets under strict i.i.d. assumptions, relying on static loss functions like standard MSE Wang and Sun [2022], Han et al. [2025], Grinsztajn et al. [2025]. However, real-world structured data is inherently heteroscedastic and heavy-tailed, populated by extreme outliers Shwartz-Ziv and Armon [2022], Borisov et al. [2024]. When exposed to this empirical variance, static optimization objectives become hypersensitive, frequently triggering gradient explosions. This fragility is severely exacerbated during large-scale, dynamic multi-task pre-training. As batch task proportions fluctuate wildly and targets are frequently missing, computing dense gradients with static weights inevitably leads to mathematical instabilities, such as division-by-zero errors and total optimization collapse.

To tackle these challenges, we propose FEAT, a linear-complexity foundation model for massive, real-world structured data. To address the first challenge, we design linear-complexity encoders for representation learning to propagate information across data samples. The model transmits contextual signals through fixed-size hidden states and attention accumulators, avoiding the construction of an $N \times N$ attention matrix and eliminating quadratic pairwise interactions. To address the second challenge, we propose a multi-layer dual-axis encoding architecture that combines two complementary encoding layers: adaptive-fusion bi-Mamba-2 (AFBM), which captures dynamic local dependencies across samples, and convolutional gated linear attention (Conv-GLA), which maintains global interactions through explicit memory accumulation. Together, these two encoding layers prevent representation collapse in linear-complexity

architectures and maintain expressive semantic representations for massive structured sequences. To address the third challenge, we propose a stable pre-training pipeline for structured data. The framework combines scale-free synthetic structural causal models (SCMs) with real-world structured datasets and employs a numerically robust Huber-based reconstruction loss. This design improves robustness to heavy-tailed noise and outliers while encouraging the model to learn stable relational patterns in structured data.

Our contributions are summarized as follows:

- We propose FEAT, the first industrial-grade structured-data foundation model built on a linear-complexity multi-layer dual-axis encoding architecture, enabling cross-sample modeling with strictly $\mathcal{O}(N)$ complexity and scalable learning on massive structured datasets.
- We design two complementary encoding layers, AFBM and Conv-GLA, to preserve expressive representations under linear modeling. AFBM captures dynamic local dependencies across samples, while Conv-GLA maintains global interactions through explicit memory accumulation, enabling robust representation learning for permutation-invariant structured data.
- We pioneer a mixed real-and-synthetic pretraining strategy fortified by a Huber-based objective. This effectively neutralizes outlier-induced gradient explosions, guaranteeing stable convergence across heteroscedastic, heavy-tailed empirical distributions and bridging the simulation-to-reality gap.
- Extensive experiments across 11 real-world benchmarks demonstrate that FEAT delivers up to a $40\times$ inference speedup at extreme context lengths (500,000 samples) compared to existing foundation models. FEAT achieves this massive computational scalability while maintaining zero-shot predictive parity with state-of-the-art baselines in both classification and regression tasks.

We review related work in Section 2 and cover preliminaries in Section 3. Section 4 introduces the objective of FEAT. Section 5 presents FEAT, while Section 6 discusses experimental findings. Section 7 concludes the paper and outlines research directions.

2 Related Work

2.1 Deep Learning for Tabular Data

Existing tabular data modeling has been dominated by tree-based ensembles Breiman [2001], Chen and Guestrin [2016], Ke et al. [2017], Prokhorenkova et al. [2018] due to their robustness against unnormalized features and irregular distributions Grinsztajn et al. [2022]. To bridge the performance gap, deep tabular models Arik and Pfister [2021], Gorishniy et al. [2021], Somepalli et al. [2021] have introduced instance-wise feature selection and tokenization. However, both paradigms strictly rely on *isolated training*—requiring exhaustive dataset-specific optimization and hyperparameter tuning from scratch. This lack of zero-shot generalization inherently restricts their scalability for task-agnostic deployment. In contrast, our proposed FEAT transcends the isolated training paradigm, acting as a universal foundation model capable of immediate, zero-shot inference across diverse and unseen structured-data environments without dataset-specific fine-tuning.

2.2 Tabular Foundation Models

Inspired by Large Language Models Brown et al. [2020], Touvron et al. [2023], recent pioneering works recast tabular prediction as an ICL task. TabPFN Hollmann et al. [2025] achieves zero-shot Bayesian inference via Prior-Data Fitted Networks, while LimiX Han et al. [2025] and TabICL Qu et al. [2025] scale context-conditional modeling to unify classification, regression, and imputation. While these LDMs show strong few-shot performance for tabular prediction, their reliance on full-attention Transformers imposes an $\mathcal{O}(N^2)$ computational complexity, which limits the context length and restricts modeling global interactions in large-scale datasets. In addition, pre-training exclusively on synthetic SCMs leads to a mismatch with real-world structured-data data, since synthetic priors fail to capture heavy-tailed empirical noise Ma et al. [2024], Zhang et al. [2025]. FEAT addresses these limitations in two ways. First, it replaces quadratic attention with a strictly $\mathcal{O}(N)$ architecture, enabling efficient processing of millions of rows. Second, it adopts a hybrid pre-training strategy that combines real and synthetic data to better align SCM-based priors with real-world data distributions.

2.3 Linear Sequence Models

To circumvent the $\mathcal{O}(N^2)$ bottleneck, linear-complexity sequence models—such as Linear Transformers Katharopoulos et al. [2020], Performers Choromanski et al. [2021], and SSMs like Mamba Gu and Dao [2024]—compress historical

context into a fixed-size state. Some methods Ahamed and Cheng [2024], Koch et al. [2025] have begun applying these to structured-data. However, standard SSMs have a causal and unidirectional inductive bias designed for sequential text. When applied to structured-data matrices, which are permutation-invariant and contain non-local feature interactions, this design introduces representation bias and weakens the modeling of global dependencies. In addition, structured-data often contains substantial noise, which further reduces the effectiveness of sequential state updates. FEAT addresses these limitations by combining AFMB with Conv-GLA. This design enables bidirectional feature modeling and improves robustness to noisy structured-data inputs, while maintaining linear complexity. As a result, FEAT supports scalable learning on large structured datasets while preserving global feature interactions.

3 Preliminaries

3.1 In-Context Learning for Structured Data

Definition 1. A *structured dataset* is typically instantiated as a data matrix $\mathbf{X} \in \mathbb{R}^{N \times D}$, where N is the number of samples and D is the number of features. Each row $\mathbf{x}_i \in \mathbb{R}^D$ represents the feature vector of the i -th sample.

Definition 2. Given a structured dataset $\mathbf{X} \in \mathbb{R}^{N \times D}$, its *label vector* is denoted as $\mathbf{y} \in \mathcal{Y}^N$, where \mathcal{Y} represents the label space and each element $y_i \in \mathcal{Y}$ corresponds to the target label of sample \mathbf{x}_i .

The label space \mathcal{Y} depends on the specific task type. For example, in classification tasks, \mathcal{Y} is a finite set of discrete class labels, while in regression tasks, \mathcal{Y} is a continuous subset of \mathbb{R} .

Definition 3. Given a structured dataset $\mathbf{X} \in \mathbb{R}^{N \times D}$ and its label vector $\mathbf{y} \in \mathcal{Y}^N$, let $\mathbf{X}_L \subset \mathbf{X}$ denote the subset of samples with observed labels $\mathbf{y}_L \subset \mathbf{y}$, and let $\mathbf{X}_U = \mathbf{X} \setminus \mathbf{X}_L$ denote the subset of query samples with unobserved labels \mathbf{y}_U . **ICL for structured data** learns a foundation model parameterized by θ to predict the label distribution of \mathbf{X}_U conditioned on \mathbf{X}_U , \mathbf{X}_L , and \mathbf{y}_L by approximating the true posterior predictive distribution:

$$P_\theta(\mathbf{y}_U \mid \mathbf{X}_U, \mathbf{X}_L, \mathbf{y}_L) \approx P(\mathbf{y}_U \mid \mathbf{X}_U, \mathbf{X}_L, \mathbf{y}_L), \quad (1)$$

where $P_\theta(\cdot)$ denotes the predictive distribution induced by the model.

At inference time, the labeled samples $(\mathbf{X}_L, \mathbf{y}_L)$ serve as the in-context support set, while \mathbf{X}_U represents the query samples. Through the in-context learning mechanism, the model directly infers the label distribution of \mathbf{X}_U based on the relational patterns observed in the support set. Since the predictive model is pre-trained to approximate the universal posterior predictive distribution, it can dynamically adapt to novel structured prediction tasks (e.g., varying feature dimensions or target types) using only the provided context, requiring absolutely no parameter updates or dataset-specific fine-tuning.

3.2 State Space Models

SSMs Gu and Dao [2024] are a class of linear-complexity sequence models that capture temporal or spatial dependencies through a continuous latent state representation. Let $t \in \mathbb{R}$ denote the continuous time (or sequence) index. Given a 1-D input signal $u(t) \in \mathbb{R}$, an SSM generates an output $y(t) \in \mathbb{R}$ by evolving a hidden state $\mathbf{h}(t) \in \mathbb{R}^{d_{state}}$ over time, where d_{state} denotes the internal state capacity.

The state evolution is governed by a continuous-time linear ordinary differential equation (ODE):

$$\mathbf{h}'(t) = \mathbf{A}\mathbf{h}(t) + \mathbf{B}u(t), \quad y(t) = \mathbf{C}\mathbf{h}(t) \quad (2)$$

Here, $\mathbf{A} \in \mathbb{R}^{d_{state} \times d_{state}}$ is the state transition matrix that dictates the system's internal dynamics, $\mathbf{B} \in \mathbb{R}^{d_{state} \times 1}$ projects the input signal into the high-dimensional latent space, and $\mathbf{C} \in \mathbb{R}^{1 \times d_{state}}$ maps the latent state back to the output space.

To enable efficient computation on discrete hardware, the continuous-time ODE must be discretized using a timescale parameter Δ (typically via the zero-order hold assumption). This transforms the continuous dynamics into a discrete-time recurrent sequence:

$$\mathbf{h}_t = \bar{\mathbf{A}}\mathbf{h}_{t-1} + \bar{\mathbf{B}}u_t, \quad y_t = \mathbf{C}\mathbf{h}_t, \quad (3)$$

where \mathbf{h}_t denotes the latent state at discrete step t , and $\bar{\mathbf{A}}$ and $\bar{\mathbf{B}}$ are the discretized matrices derived from \mathbf{A} , \mathbf{B} , and Δ .

This recurrent formulation allows SSMs to process sequences with $\mathcal{O}(N)$ linear time complexity and constant memory. However, standard SSMs based on Equation (3) are inherently unidirectional and causal, which presents a fundamental structural challenge when applied to permutation-invariant structured data.

4 Problem Statement

4.1 The Dual Bottlenecks of Structured-Data Foundation Models

Existing structured-data foundation models follow the ICL paradigm defined in Def. 3. Given a structured dataset $\mathbf{X} \in \mathbb{R}^{N \times D}$ and a partially observed label vector \mathbf{y} , the model receives labeled samples $(\mathbf{X}_L, \mathbf{y}_L)$ as context and predicts the labels of the remaining samples \mathbf{X}_U . To enable context-conditioned reasoning, most existing large structured-data models first embed each data entry and construct a sequence representation of the input samples. Specifically, each feature vector \mathbf{x}_i is mapped to a feature embedding of dimension d , producing a tensor representation $\mathcal{X} \in \mathbb{R}^{N \times D \times d}$, where N denotes the number of samples and D the number of features. Some structured-data foundation models further apply full Transformer self-attention along the sample dimension N to capture cross-sample interactions. However, this global pairwise computation incurs quadratic complexity in the sequence length, resulting in a time and memory cost of $\mathcal{O}_{attn} = \mathcal{O}(N^2 \cdot D \cdot d)$.

As the dataset size increases, this quadratic scaling quickly becomes a fundamental bottleneck, preventing the model from handling long contexts or large-scale structured datasets.

To address this limitation, one natural direction is to replace attention with linear sequence models such as SSMs, which reduce the computational complexity to $\mathcal{O}(N)$. However, directly applying sequential state-space models to structured data introduces several fundamental representation issues that have been largely overlooked.

Bottleneck 1: The Linear Trap in Structured Data. Linear sequence models summarize all historical information into a fixed-size hidden state $\mathbf{h}_i \in \mathbb{R}^{d_{state}}$. For long structured sequences with heterogeneous samples and high noise levels, this constrained state representation forces the model to compress large amounts of information into a limited capacity. As the sequence grows, useful signals are gradually diluted by noise, leading to progressive information decay and a severe degradation of the signal-to-noise ratio.

Bottleneck 2: Causal Mask Deficit in Structured Data. Unlike tokens in natural language, samples in a structured dataset do not possess an intrinsic temporal ordering, and their representation should therefore be permutation-invariant. Sequential SSMs, however, process inputs in a strictly ordered manner and implicitly impose a lower-triangular causal mask over the sequence. When structured samples are arranged in an arbitrary order, this artificial causality restricts information flow and prevents early-indexed samples from accessing forward contextual information. As a result, the model cannot fully capture global relationships across samples, leading to biased and sub-optimal representations.

4.2 Objective of FEAT

FEAT aims to learn a zero-shot in-context foundation model with linear complexity for massive structured sequences. Its objective is to learn a mapping function f_θ that predicts the label distribution of unlabeled samples from labeled in-context examples, while requiring no task-specific parameter updates during inference. Different from existing Transformer-based structured-data foundation models, FEAT is developed to break the $\mathcal{O}_{attn} = \mathcal{O}(N^2 \cdot D \cdot d)$ memory wall induced by full self-attention. Different from standard linear sequence models, FEAT is further designed to avoid two key bottlenecks in structured sequence modeling: excessive hidden-state compression, which limits long-range information preservation, and artificial unidirectional ordering, which violates the permutation-invariant nature of structured data. In this way, FEAT seeks to provide a zero-shot ICL model that scales linearly with the number of samples, preserves global cross-sample dependencies, and supports multiple downstream tabular prediction tasks.

5 FEAT

5.1 Overview of FEAT

As shown in Fig. 1, FEAT consists of three main components: cell-level embedding, multi-layer dual-axis encoding, and task-aware prediction.

Cell-level embedding. Given a structured dataset $\mathbf{X} \in \mathbb{R}^{N \times D}$, FEAT first projects each data cell into a dense embedding space and converts the raw input into a 3D tensor $\mathcal{X}^{(0)} \in \mathbb{R}^{N \times D \times d}$, where N is the number of samples, D is the number of features, and d is the embedding dimension. This representation preserves both the sample-wise and feature-wise organization of structured data, serving as the foundation for subsequent dual-axis representation learning. The detailed embedding process is described in Section 5.2.

Multi-layer dual-axis encoding. The tensor $\mathcal{X}^{(0)}$ is then processed by L stacked FEAT blocks, each of which decomposes structured-data representation learning into two sequential modeling stages: *Feature-axis modeling* and

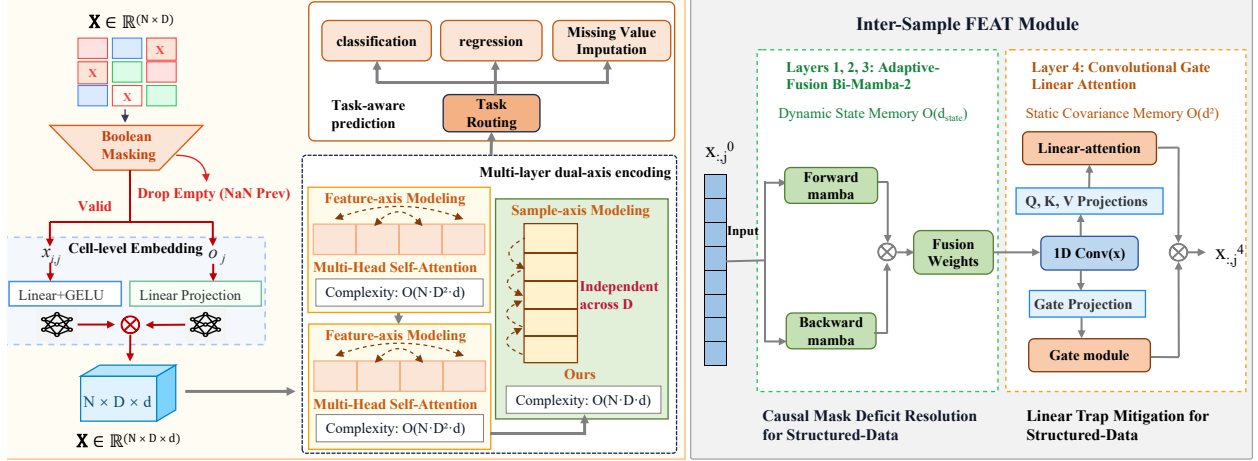


Figure 1: The overview of FEAT.

Sample-axis modeling. The feature-axis modeling stage models intra-sample feature dependencies by applying self-attention across the D feature columns of each sample, efficiently capturing local semantic correlations. The sample-axis modeling stage then models inter-sample dependencies along the sample dimension using a linear-complexity modeling mechanism, enabling efficient long-range cross-sample interaction modeling. The detailed architecture of the dual-axis encoding blocks is presented in Section 5.3.

Task-aware prediction. After passing through the stacked FEAT blocks, the resulting contextualized representations are used to predict the labels of unlabeled samples conditioned on the labeled in-context examples. This design enables FEAT to perform zero-shot ICL across multiple structured-data prediction tasks, including classification and regression. The task prediction mechanism is described in Section 5.4.

Pre-training. To enable zero-shot generalization across diverse structured-data tasks, FEAT is pre-trained on a large corpus of synthetic structured datasets generated by an advanced hybrid SCM pipeline. During training, FEAT follows a context-conditional masked modeling paradigm and jointly optimizes feature reconstruction and task prediction objectives. The detailed pre-training procedure is described in Section 5.5.

5.2 Cell-level Embedding

Unlike natural language, structured data $\mathbf{X} \in \mathbb{R}^{N \times D}$ is characterized by strict permutation invariance along both the sample axis and the feature axis. Flattening such data into 1D sequences intrinsically corrupts this structural independence. To process this natively, FEAT transforms raw data cells $x_{i,j}$ into a 3D contextual tensor $\mathcal{X}^{(0)} \in \mathbb{R}^{N \times D \times d}$ using two independent, additive embeddings: a value projection and a column-axis feature identifier.

First, we uniquely map continuous scalar values to a d -dimensional semantic space. The structured data is encoded via a non-linear MLP, while missing or intentionally masked values (during pre-training) are substituted with a shared learnable token. Formally, the embedding $e_{i,j}^{val}$ for the cell at row i and column j in \mathbf{X} is computed as:

$$e_{i,j}^{val} = \begin{cases} \text{MLP}(x_{i,j}), & \text{if } x_{i,j} \text{ is observed,} \\ \mathbf{m}_{mask}, & \text{if } x_{i,j} \text{ is missing or masked.} \end{cases} \quad (4)$$

Where $\text{MLP}(\cdot)$ is the linear MLP model and $\mathbf{m}_{mask} \in \mathbb{R}^d$ is the shared learnable token.

Then, we apply standard positional encodings across the feature dimension to impose a false geometric distance bias. To strictly preserve column permutation invariance, FEAT introduces subspace orthogonal discriminative feature encoding (S-DFE). Instead of learning static positional mappings, S-DFE dynamically provides equidistant feature identities.

In each forward pass, we randomly sample a low-rank orthogonal matrix $\mathbf{O} \in \mathbb{R}^{D \times \frac{d}{4}}$, where each row vector $\mathbf{o}_j \in \mathbb{R}^{\frac{d}{4}}$ serves as the base identity for the j -th column. The pairwise orthogonality ($\mathbf{o}_j^\top \mathbf{o}_k = 0$ for $j \neq k$) guarantees that every feature is distinctly identifiable yet perfectly equidistant in the subspace, eliminating any associative ordering bias. This identity signature is then linearly projected to the hidden dimension d via a learnable weight matrix $\mathbf{W}_{dfe} \in \mathbb{R}^{\frac{d}{4} \times d}$:

$$\text{loc}_j^{col} = \mathbf{o}_j \mathbf{W}_{dfe} \quad (5)$$

This dynamic strategy allows FEAT to effectively model columns purely based on their distinct identities, achieving inherent zero-shot adaptability on unseen structured datasets with arbitrary schemas.

The final cell representation $\mathcal{X}_{i,j}^{(0)}$ is obtained by element-wise aggregating the data projection and the column-axis identifier, followed by layer normalization for stable optimization:

$$\mathcal{X}_{i,j}^{(0)} = \text{LayerNorm} \left(\mathbf{e}_{i,j}^{val} + \mathbf{loc}_j^{col} \right) \quad (6)$$

This fusion yields a rich, structurally preserved 3D matrix $\mathcal{X}^{(0)}$, which serves as the contextual foundation for the dual-axis modeling blocks.

5.3 Multi-layer dual-axis encoding

Following the initial embedding stage, the 3D tensor $\mathcal{X}^{(0)} \in \mathbb{R}^{N \times D \times d}$ is processed by L stacked dual-axis encoding blocks. Each encoding block consists of two feature axis modeling and one sample axis modeling. To effectively capture both local attribute correlations and global context without suffering from computationally prohibitive dense attention over the flattened $N \times D$ sequence, each block $l \in \{1, \dots, L\}$ factorizes the representation learning into two orthogonal stages: Feature-axis modeling and Sample-axis modeling.

5.3.1 Feature-axis Modeling

The primary objective of the feature-axis modeling stage is to model the intra-sample dependencies (i.e., interactions among different features within the same sample). Because features in structured data often exhibit complex, non-linear correlations, we employ multi-head self-attention (MHSA) across the feature dimension D .

For the l -th block, given the input tensor $\mathcal{X}^{(l-1)} \in \mathbb{R}^{N \times D \times d}$, we strictly isolate the computations across the sample axis (N). For each independent sample index $i \in \{1, \dots, N\}$, we extract its corresponding 2D feature matrix $\mathbf{F}_i^{(l-1)} = \mathcal{X}_{i,:}^{(l-1)} \in \mathbb{R}^{D \times d}$. The routing is then defined by standard Transformer layer operations—comprising MHSA and a Feed-Forward Network (FFN), interleaved with Layer Normalization (LN) and residual connections:

$$\tilde{\mathbf{F}}_i^{(l-1)} = \mathbf{F}_i^{(l-1)} + \text{MHSA} \left(\text{LN}(\mathbf{F}_i^{(l-1)}) \right), \quad (7)$$

$$\hat{\mathbf{F}}_i^{(l-1)} = \tilde{\mathbf{F}}_i^{(l-1)} + \text{FFN} \left(\text{LN}(\tilde{\mathbf{F}}_i^{(l-1)}) \right). \quad (8)$$

The operation is strictly constrained within the D tokens of sample i . The MHSA mechanism aggregates information from all D columns to contextualize each specific feature representation, seamlessly updating the value embeddings based on the S-DFE identities introduced in the previous stage.

Finally, the independently processed matrices $\hat{\mathbf{F}}_i^{(l-1)}$ for all N samples are stacked back together to form the intermediate 3D tensor $\hat{\mathcal{X}}^{(l-1)} \in \mathbb{R}^{N \times D \times d}$, which serves as the direct input to the Sample-axis routing stage.

5.3.2 Sample-Axis Modeling

To simultaneously address the *linear trap* and the *causal mask deficit* while maintaining linear computational complexity, FEAT introduces a heterogeneous sequence modeling architecture along the sample dimension. Instead of relying on a single sequential module, FEAT integrates two complementary mechanisms: AFBM which captures dynamic local dependencies across samples, and Conv-GLA which provides stable global memory over arbitrarily long sequences.

Specifically, the sample-axis modeling stage consists of four continuous layers arranged in a fixed topology: three AFBM layers ($l \in \{1, 2, 3\}$) followed by one Conv-GLA layer ($l = 4$). The AFBM layers perform efficient bidirectional sequence modeling to extract local inter-sample dynamics while mitigating the causal mask deficit of standard SSMs. However, since state-space models inherently compress historical information into bounded hidden states, they remain susceptible to the linear trap when the sequence length becomes extremely large. To alleviate this limitation, the Conv-GLA layer introduces an explicit global memory reservoir that stores long-range dependencies without forcing excessive compression into the hidden state.

AFBM. For an input representation $\hat{\mathcal{X}}_{i,j}^{(l-1)} \in \mathbb{R}^d$, the model computes forward and backward state transitions:

$$\vec{\mathbf{h}}_{i,j}^{(l)} = \bar{\mathbf{A}}^{(l)} \vec{\mathbf{h}}_{i-1,j}^{(l)} + \bar{\mathbf{B}}^{(l)} \hat{\mathcal{X}}_{i,j}^{(l-1)}, \quad (9)$$

$$\overleftarrow{\mathbf{h}}_{i,j}^{(l)} = \text{Mamba-Bwd} \left(\hat{\mathcal{X}}_{i,j}^{(l-1)} \right), \quad (10)$$

where $\vec{\mathbf{h}}_{i,j}^{(l)}, \overleftarrow{\mathbf{h}}_{i,j}^{(l)} \in \mathbb{R}^{d_{state}}$ represent the forward and backward hidden states, respectively, for the j -th feature of the i -th sample at the l -th layer. $\bar{\mathbf{A}}^{(l)} \in \mathbb{R}^{d_{state} \times d_{state}}$ and $\bar{\mathbf{B}}^{(l)} \in \mathbb{R}^{d_{state} \times d}$ denote the discretized state transition and

input projection matrices derived from the continuous SSM dynamics. $\text{Mamba-Bwd}(\cdot)$ indicates the identical Mamba-2 state-space operation computed in the reverse sequence order (from sample $i = N$ down to 1).

The two directional states are fused via a learnable projection:

$$\mathcal{X}_{i,j}^{(l)} = \mathbf{W}_{fuse}^{(l)} \left[\vec{\mathbf{h}}_{i,j}^{(l)} \parallel \overleftarrow{\mathbf{h}}_{i,j}^{(l)} \right], \quad (11)$$

where $\mathcal{X}_{i,j}^{(l)} \in \mathbb{R}^d$ is the fused contextual representation. The operator $[\cdot \parallel \cdot]$ denotes vector concatenation along the hidden state dimension, yielding a combined bidirectional state in $\mathbb{R}^{2d_{state}}$. $\mathbf{W}_{fuse}^{(l)} \in \mathbb{R}^{d \times 2d_{state}}$ is the learnable weight matrix responsible for projecting the concatenated state back to the original embedding dimension d .

This bidirectional fusion removes the artificial causality imposed by standard SSMs and enables permutation-aware feature extraction across samples. Nevertheless, since AFBM still relies on bounded hidden states of size $\mathcal{O}(d_{state})$, its capacity for storing long-range information remains limited when the sequence length grows very large.

Conv-GLA. Unlike standard linear attention that indiscriminately aggregates all samples and amplifies noise, Conv-GLA first applies localized smoothing before constructing global memory. Specifically, a 1D convolution acts as a low-pass filter over the output of the third AFBM layer:

$$\tilde{\mathcal{X}}_{i,j}^{(3)} = \text{Conv1D}\left(\mathcal{X}_{i,j}^{(3)}, \text{kernel_size} = K\right), \quad (12)$$

where $\tilde{\mathcal{X}}_{i,j}^{(3)} \in \mathbb{R}^d$ is the smoothed feature representation, $\mathcal{X}_{i,j}^{(3)}$ is the output from the final ($l = 3$) AFBM layer, and K denotes the kernel size of the 1D depthwise convolution applied along the sample dimension N to aggregate local context and attenuate high-frequency noise.

We then obtain the key and value vectors via linear projections: $\mathbf{k}_{i,j} = \mathbf{W}_k \tilde{\mathcal{X}}_{i,j}^{(3)}$ and $\mathbf{v}_{i,j} = \mathbf{W}_v \tilde{\mathcal{X}}_{i,j}^{(3)}$, where $\mathbf{W}_k, \mathbf{W}_v \in \mathbb{R}^{d \times d}$. A data-dependent gating mechanism modulates the value vectors:

$$\mathbf{g}_{i,j} = \text{SiLU}(\mathbf{W}_g \tilde{\mathcal{X}}_{i,j}^{(3)}), \quad \tilde{\mathbf{v}}_{i,j} = \mathbf{g}_{i,j} \odot \mathbf{v}_{i,j}, \quad (13)$$

where $\mathbf{g}_{i,j} \in (0, 1)^d$ is the dynamic gating vector that evaluates the informativeness of the current sample. $\mathbf{W}_g \in \mathbb{R}^{d \times d}$ is the learnable gating projection matrix, $\text{SiLU}(\cdot)$ is the sigmoid linear unit activation function used to ensure smooth, non-linear gating probabilities, and \odot denotes the element-wise (Hadamard) product.

The gated values are accumulated into a covariance memory matrix:

$$\mathbf{S}_{i,j} = \mathbf{S}_{i-1,j} + \phi(\mathbf{k}_{i,j}) (\mathbf{g}_{i,j} \odot \mathbf{v}_{i,j})^\top, \quad (14)$$

where $\mathbf{S}_{i,j} \in \mathbb{R}^{d \times d}$ is the accumulated global covariance memory matrix at step i , summarizing all historical key-value interactions for the j -th feature. $\phi(\cdot)$ is a non-linear kernel mapping function applied to the key vectors to maintain positive semi-definiteness, and \top denotes the vector transpose operation forming the outer product between the mapped key and the gated value.

By adaptively suppressing uninformative samples ($\mathbf{g}_{i,j} \rightarrow 0$), the variance of the accumulated memory remains bounded, ensuring stable global context modeling even for extremely long sequences.

This carefully designed heterogeneous topology explicitly decouples aggressive local noise filtering (handled by the dynamic state memory of AFBM) from global long-range storage (handled by the static covariance memory of Conv-GLA). As a result, FEAT achieves scalable long-context modeling while avoiding both representation collapse and sequence-length degradation.

5.4 Task-aware prediction

After the dual-axis representation learning across the L stacked FEAT blocks, the network outputs a final contextualized 3D tensor $\mathcal{X}^{(L)} \in \mathbb{R}^{N \times (D+1) \times d}$. The sequence dimension expands to $D + 1$ because a unified label token, acting as the target variable prompt, is appended to the D feature tokens of each sample. For the labeled context samples in \mathbf{X}_L , this token encodes the ground-truth label \mathbf{y}_L ; For the unlabeled query samples in \mathbf{X}_U , it is initialized as a learnable mask embedding.

To support both downstream zero-shot prediction and self-supervised pre-training simultaneously, FEAT decouples the decoding process into three task-specific heads. We first extract the task-relevant hidden states from $\mathcal{X}^{(L)}$ for the query

samples $i \in \{N_L + 1, \dots, N\}$, where $N_L = |\mathbf{X}_L|$ is the number of in-context examples:

$$\text{Target state: } \mathbf{z}_i^y = \mathcal{X}_{i,D+1,:}^{(L)} \in \mathbb{R}^d \quad (15)$$

$$\text{Feature states: } \mathbf{z}_{i,j}^x = \mathcal{X}_{i,j,:}^{(L)} \in \mathbb{R}^d, \quad \forall j \in \{1, \dots, D\} \quad (16)$$

The target state \mathbf{z}_i^y fundamentally aggregates both intra-sample feature dependencies and inter-sample supervision signals, while the feature states $\mathbf{z}_{i,j}^x$ capture the contextualized semantic representation of individual structured attributes. FEAT dynamically routes these states to the corresponding prediction heads, utilizing parallel MLPs with tailored architectures. For all following MLPs, we denote d_{hidden} as the intermediate hidden projection dimension, and bias terms are omitted for notational brevity:

Classification head. For classification tasks with a finite label space of size C , the target state \mathbf{z}_i^y is mapped to class logits via a two-layer network with a GELU activation Hendrycks and Gimpel [2016]:

$$\hat{\mathbf{y}}_i = \mathbf{W}_{c2}(\text{GELU}(\mathbf{W}_{c1}\mathbf{z}_i^y)) \in \mathbb{R}^C \quad (17)$$

where $\mathbf{W}_{c1} \in \mathbb{R}^{d_{\text{hidden}} \times d}$ and $\mathbf{W}_{c2} \in \mathbb{R}^{C \times d_{\text{hidden}}}$ are the learnable projection weights. The predicted categorical distribution approximates the true posterior $P_\theta(\mathbf{y}_U | \mathbf{X}_U, \mathbf{X}_L, \mathbf{y}_L)$ as defined in Eq. 1 via Softmax normalization.

Regression head. For continuous regression tasks, predicting unscaled scalar values is highly susceptible to explosive variance. Thus, we integrate Layer Normalization within the hidden projection to strictly bound the activation magnitude before computing the final scalar output:

$$\hat{y}_i = \mathbf{W}_{r2}(\text{GELU}(\text{LayerNorm}(\mathbf{W}_{r1}\mathbf{z}_i^y))) \in \mathbb{R} \quad (18)$$

where $\mathbf{W}_{r1} \in \mathbb{R}^{d_{\text{hidden}} \times d}$ and $\mathbf{W}_{r2} \in \mathbb{R}^{1 \times d_{\text{hidden}}}$ parameterize the regression MLP to output a continuous scalar.

Missing value imputation head (MVIH). To serve the context-conditional masked modeling (CCMM) pre-training objective and perform missing data imputation dynamically, FEAT must reconstruct the masked features. The feature state $\mathbf{z}_{i,j}^x$ is transformed back into the original numerical feature space using a stabilized architecture homologous to the regression head:

$$\hat{x}_{i,j} = \mathbf{W}_{f2}(\text{GELU}(\text{LayerNorm}(\mathbf{W}_{f1}\mathbf{z}_{i,j}^x))) \in \mathbb{R} \quad (19)$$

where $\mathbf{W}_{f1} \in \mathbb{R}^{d_{\text{hidden}} \times d}$ and $\mathbf{W}_{f2} \in \mathbb{R}^{1 \times d_{\text{hidden}}}$ represent the projection matrices specifically tailored for instance-level feature reconstruction.

This decoupled multi-head decoding strategy enables FEAT to perform seamless zero-shot downstream inference while simultaneously providing robust self-supervised feature reconstruction. By relying purely on the unified structural representations conditioned on the implicitly retrieved rules from the labeled context \mathbf{X}_L , the model circumvents any requirement for task-specific parameter updates or architecture modifications at inference time.

5.5 Pre-training

5.5.1 Hybrid SCM Generation Pipeline

While existing large structured-data models pre-train on synthetic SCM, their hierarchical Directed Acyclic Graphs (DAGs) typically generate homogeneous structures with independent, identically distributed (i.i.d.) root variables. Such assumptions fail to reflect the statistical complexities of real-world structured-data domains. To synthesize training corpora $\mathbf{X} \in \mathbb{R}^{N \times D}$ and labels \mathbf{y} that better match the dual-axis modeling capacity of FEAT, we introduce an advanced hybrid SCM generation pipeline. This pipeline progressively incorporates realistic structural variations and non-stationary statistical characteristics through four rigorous steps.

(i) Scale-free causal graph generation. Standard generators use uniform edge sampling, which ignores feature importance disparities. Instead, we construct the DAG topology $G = (V, E)$ over D nodes using a preferential attachment mechanism. This yields a scale-free topology, allowing certain variables to emerge as highly connected "hubs." This design directly mimics the behavior of universal confounders in real-world datasets (e.g., "Age" or "Income"), which intrinsically dictate the distribution of numerous downstream variables.

(ii) Prototype-based root initialization. Let $V_{\text{root}} \subset V$ denote the set of D_{root} root nodes (in-degree of 0). To break the conventional i.i.d. assumption and explicitly introduce multi-modal row correlations, we assume the existence of

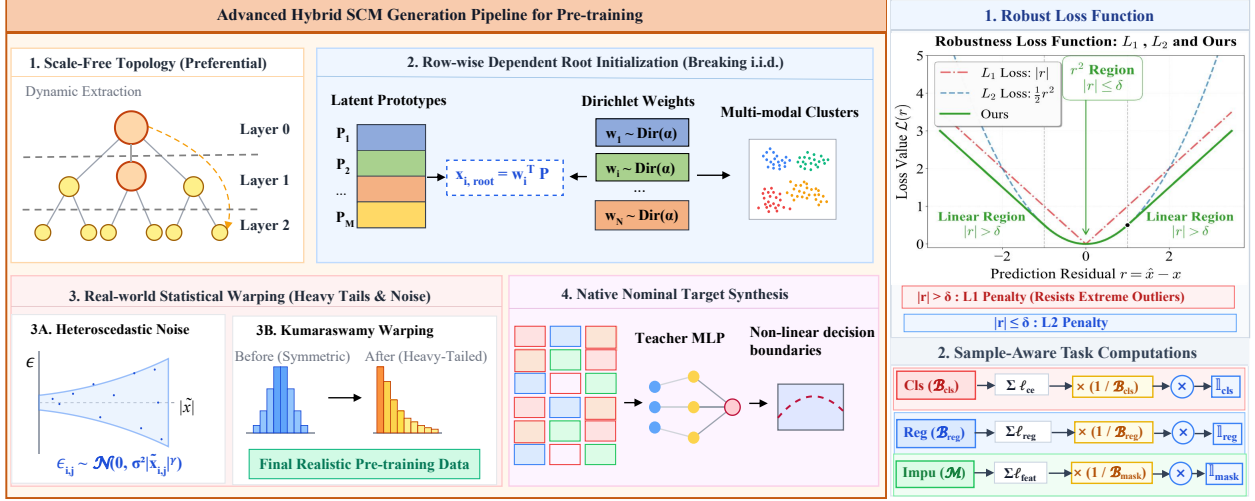


Figure 2: Pre-training methods of FEAT.

M latent prototypes $\mathbf{P} \in \mathbb{R}^{M \times D_{root}}$ representing underlying population clusters. For each sample $i \in \{1, \dots, N\}$, we draw an individual mixture weight vector from a Dirichlet distribution $\mathbf{w}_i \sim \text{Dir}(\alpha)$. The root features are then synthesized as:

$$\mathbf{x}_{i,root} = \mathbf{w}_i^\top \mathbf{P} \in \mathbb{R}^{D_{root}} \quad (20)$$

This explicitly injects sample-wise clustering structures commonly observed in structured patient/user profiles.

(iii) Causal propagation with heteroscedastic noise. For every continuous non-root node $j \in V \setminus V_{root}$, its intermediate value $\tilde{x}_{i,j}$ is propagated via a non-linear causal mechanism f_j acting on its parent variables. We denote this set of parent variables as $\text{Pa}(j)$. Specifically, the intermediate representation is computed as $\tilde{x}_{i,j} = f_j(\mathbf{x}_{i,\text{Pa}(j)})$. To simulate measurement flaws and value-dependent uncertainties, we abandon static Gaussian noise and introduce exponential heteroscedastic noise. The final variable value is modified as:

$$x_{i,j} = \tilde{x}_{i,j} + \epsilon_{i,j}, \quad \text{where } \epsilon_{i,j} \sim \mathcal{N}(0, \sigma^2 |\tilde{x}_{i,j}|^\gamma) \quad (21)$$

where γ explicitly scales the noise variance with the magnitude of the signal, a hallmark of heavily skewed real-world metrics.

(iv) Nominal target synthesis & marginal warping. To generate the final target labels y_i , we eschew the naive ordinal binning used in prior works. Instead, we employ a native nominal synthesis process where a sparse teacher MLP queries the intermediate causal representations explicitly to compute target logits. By stochastically modulating the Signal-to-Noise Ratio in these logits, this procedure inherently produces highly non-linear, heterogeneous decision boundaries mapping to regression or classification tasks.

Finally, to faithfully emulate heavy-tailed outliers, we apply stochastic Kumaraswamy warping to the continuous variables. This transformation skews the marginal feature distributions toward heavy-tailed domains while precisely preserving the monotonic ranking and dependencies implied by the causal structure.

Together, these sequentially applied structural and statistical innovations synthesize a fundamentally rigorous pre-training corpus, substantially narrowing the reality gap between synthetic SCM arrays and naturally occurring structured-data distributions.

5.5.2 Loss Function

Following the context-conditional masked modeling paradigm, the pre-training objective of FEAT jointly optimizes feature reconstruction and task prediction. To ensure numerical stability under heavy-tailed structured-data distributions and highly variable context lengths, the optimization pipeline incorporates robust measurement mechanisms and a dynamic loss balancing strategy.

For the self-supervised feature reconstruction objective, we adopt the Smooth L1 loss rather than the standard mean squared error (MSE). Structured data frequently contains extreme outliers manifesting from heavy-tailed distributions, which inadvertently trigger exploding gradients when penalized squarely. The Huber mechanism acts as an L2 penalty for minor reconstruction errors while smoothly transitioning to an L1 penalty for severe deviations. Let \mathcal{M} denote the set of masked cell coordinates (i, j) in a given batch, where $i \in \{1, \dots, N\}$ indexes the sample and $j \in \{1, \dots, D\}$

indexes the feature column. For a predicted feature value $\hat{x}_{i,j}$ and its underlying ground truth $x_{i,j}$, the localized reconstruction loss is defined as:

$$\ell_{feat}^{(i,j)} = \begin{cases} \frac{1}{2}(\hat{x}_{i,j} - x_{i,j})^2 & \text{for } |\hat{x}_{i,j} - x_{i,j}| \leq \delta, \\ \delta|\hat{x}_{i,j} - x_{i,j}| - \frac{1}{2}\delta^2 & \text{otherwise,} \end{cases} \quad (22)$$

where $\delta > 0$ is a strict threshold hyperparameter governing the transition regime between squared and absolute absolute penalty scales.

To further stabilize the optimization space across heterogeneous downstream semantics, we enforce a dynamic loss balancing strategy. Because each synthesized multi-task batch contains radically fluctuating proportions of classification samples, regression samples, and masked features, assigning static scalar weights inevitably results in gradient domination or representation collapse. To counteract this, the overall loss aggregates each task-specific objective averaged strictly over its valid samples.

We define \mathcal{B}_{cls} and \mathcal{B}_{reg} as the varying sets of sample indices i natively apportioned to classification and regression tasks in the current batch. The dynamically balanced total loss objective is aggregated as:

$$\begin{aligned} \mathcal{L}_{total} = & \mathbb{I}_{cls} \left(\frac{1}{|\mathcal{B}_{cls}|} \sum_{i \in \mathcal{B}_{cls}} \ell_{ce}^{(i)} \right) + \mathbb{I}_{reg} \left(\frac{1}{|\mathcal{B}_{reg}|} \sum_{i \in \mathcal{B}_{reg}} \ell_{reg}^{(i)} \right) \\ & + \mathbb{I}_{mask} \left(\frac{1}{|\mathcal{M}|} \sum_{(i,j) \in \mathcal{M}} \ell_{feat}^{(i,j)} \right), \end{aligned} \quad (23)$$

where $\ell_{ce}^{(i)}$ calculates the standard cross-entropy penalty given categorical probabilities, and $\ell_{reg}^{(i)}$ leverages a task-level Huber objective homologous to Eq. 22 for stable continuous target optimization. Functionally, $|\mathcal{B}_{cls}|$, $|\mathcal{B}_{reg}|$, and $|\mathcal{M}|$ express the absolute cardinality of their specific valid domains. The indicator functions $\mathbb{I}_{cls}, \mathbb{I}_{reg}, \mathbb{I}_{mask} \in \{0, 1\}$ operate as computational logical switches—intelligently activating specific loss modules exclusively when their pertinent sets evaluate as non-empty during the stochastic sampling batch.

Finally, to preclude numeric saturation endemic to natively sporadic structured templates, precise boolean verification arrays explicitly mask any missing data cells ahead of arithmetic projection. This protocol comprehensively ensures that intrinsic ‘NaN’ or ‘Inf’ artifacts never taint the gradient trajectories traversing throughout arbitrary length resolutions.

6 Experiment

To rigorously evaluate the proposed FEAT framework, our experiments are designed to answer two fundamental research questions (RQs):

- **RQ1 (Scalability & Efficiency):** Does the FEAT empirically deliver the mathematically promised $\mathcal{O}(N)$ linear scaling, and how does it compare against the $\mathcal{O}(N^2)$ memory wall of standard sequence-based structured-data models?
- **RQ2 (Predictive Parity):** Can FEAT maintain competitive zero-shot predictive performance across diverse real-world datasets without succumbing to the representation collapse typical of linear sequence models?

6.1 Experimental Setup

Baselines. We benchmark FEAT against a comprehensive suite of state-of-the-art structured-data learning models, spanning modern foundation models, automated machine learning (AutoML), and classical gradient boosting. From a feature-representation perspective, these baselines are categorized as follows:

- **Limix** [Han et al., 2025] employs a full Transformer architecture with asymmetric self-attention to model the joint distribution of structured features.
- **TabICL v2** [Qu et al., 2025] is an advanced in-context learning foundation model that handles massive contexts via a two-stage embedding pipeline. It first captures statistical properties through distribution-aware column-wise embeddings, followed by row-wise attention to model cross-feature dependencies.
- **TabPFN Suite** [Hollmann et al., 2025, Grinsztajn et al., 2025, Garg et al., 2025] employs Transformer-based prior-data fitted networks (PFNs) pre-trained on synthetic structural causal models for zero-shot inference. In our experiments, we evaluate TabPFN 2.5, which supports larger feature and context dimensions, and TabPFN-Real, which further benefits from continued pre-training on real-world datasets to improve feature generalization.

- **AutoGluon v1.5** [Erickson et al., 2020] is a state-of-the-art AutoML framework that automates robust feature engineering (e.g., scaling, imputation) and constructs multi-layer stack ensembles of diverse traditional and deep models, representing the upper bound of classical supervised learning.
- **CatBoost** [Prokhorenkova et al., 2018] is a gradient boosting framework optimized for categorical features. It employs an ordered boosting scheme and target statistics to prevent target leakage and prediction shift during feature conversion.
- **LightGBM** [Ke et al., 2017] is an efficient tree-boosting system that uses gradient-based one-side sampling (GOSS) and exclusive feature bundling (EFB) to handle high-dimensional and sparse feature spaces efficiently.
- **XGBoost** [Chen and Guestrin, 2016] is a scalable tree-boosting framework that employs sparsity-aware split finding to automatically handle missing feature values and uses a block structure for parallel computation.

Benchmark Datasets. To rigorously evaluate predictive parity (RQ2) and ensure our model handles diverse structured regimes, we follow the robust evaluation protocol established in recent structured-data foundation studies [Han et al., 2025]. We utilize 11 heterogeneous datasets from the following standard benchmarking suites:

- **TabPFN Suite** (`pfn_cls`, `pfn_reg`) [Hollmann et al., 2025]: A rigorous suite of small-to-medium scale datasets designed to test zero-shot in-context generalization across unseen feature spaces.
- **Tabzilla Benchmark** (Tabzilla-CLS) [McElfresh et al., 2023]: A massive, highly diverse collection of structured-data classification tasks. It serves as a comprehensive stress test for algorithmic robustness, evaluating performance across wildly varying domain origins, feature complexities, and class imbalances.
- **TALENT Benchmark** (`talent_cls_benchmark`, `talent_reg_benchmark`) [Liu et al., 2025]: A comprehensive aggregation of diverse real-world structured-data tasks, serving as a primary testbed for feature interaction robustness.
- **TabArena Benchmark** (`tabarena_cls_benchmark`, `tabarena_reg_benchmark`) [Erickson et al., 2025]: A modern, highly challenging evaluation suite featuring complex structural schemas, class imbalances, and mixed data types.
- **LimiX Curated Suites** (BCC0, CTR23) [Han et al., 2025]: To evaluate scalability and domain shift, we adopt the specific dataset partitions curated by LimiX. This includes the **BCC0 Suite** for high-cardinality signal-to-noise testing, **CTR23** for massive-scale extreme sparsity recommendation environments.
- **GI Benchmark** (`gi_cls`, `gi_reg`): A proprietary, real-world industrial dataset suite sourced from internal production environments. It encompasses highly heterogeneous structured data spanning diverse sectors, including finance, gaming, and consumer goods. This benchmark serves as a rigorous testbed to evaluate the model’s cross-industry generalization and robustness on complex, production-grade data.

Metrics. Computational efficiency (RQ1) is evaluated via end-to-end inference latency (ms). Downstream predictive performance (RQ2) is measured using the area under the receiver operating characteristic curve (AUC), accuracy (ACC), and F1-score for classification tasks. For regression tasks, performance is evaluated using the root mean squared error (RMSE) and the coefficient of determination (R^2 Score). Detailed hardware configurations and hyperparameter settings are provided in Appendix 9.

6.2 Scalability and Efficiency Evaluation

Table 1: Inference Latency (ms) ($D = 20$), where (i) the best performance is marked in bold and (ii) - denotes kernel error on a 140GB GPU.

Context Size	Model			
	FEAT	TabICL v2	LimiX	TabPFN
5,000	149.15 ± 0.97	167.23 ± 35.56	197.76 ± 1.02	4287.81 ± 35.22
10,000	240.13 ± 0.22	281.27 ± 62.39	391.08 ± 8.02	4495.67 ± 39.61
20,000	368.46 ± 1.55	404.80 ± 43.34	946.13 ± 9.01	7673.87 ± 45.18
50,000	332.76 ± 2.24	608.84 ± 233.05	6540.54 ± 53.35	9412.49 ± 36.98
100,000	399.07 ± 0.79	1307.57 ± 438.59	-	-
200,000	444.80 ± 1.36	4287.77 ± 906.45	-	-
300,000	486.73 ± 9.16	8609.52 ± 854.87	-	-
400,000	529.50 ± 10.24	14856.98 ± 788.68	-	-
500,000	564.53 ± 9.07	22498.94 ± 1036.45	-	-

We evaluate the efficiency of FEAT by measuring inference latency under progressively increasing sample lengths N , while fixing the feature dimension to $D = 20$ and compare FEAT with TabICL v2, LimiX, and TabPFN under extremely large context sizes. The results in Table 1 show that the inference latency of full-attention models grows rapidly as the sample size increases. When the context expands from 5,000 to 50,000 samples, the latency of LimiX increases from 197.76 ms to 6540.54 ms, while TabPFN already exhibits high baseline latency. When further scaling the context window to 500,000 samples, TabICL v2 experiences severe slowdown, with inference time exceeding 22 seconds. In contrast, FEAT maintains stable latency growth, increasing from 153.01 ms to 564.53 ms even when the context expands from 5,000 to 500,000 samples. This is because existing baselines rely on quadratic self-attention whose computation and memory costs grow rapidly with the number of samples, whereas FEAT performs cross-sample modeling with linear-complexity operators, enabling stable inference under both higher feature dimensions and extremely large contexts.

6.3 Predictive Performance Evaluation

Table 2: Classification benchmark results, where the best performance is marked in bold.

Method	AUC	ACC	F1	Method	AUC	ACC	F1
BCCO-CLS				GI-CLS			
FEAT	0.8579	0.7719	0.6916	FEAT	0.8991	0.8698	0.6786
LimiX	0.8628	0.7892	0.7056	LimiX	0.8810	0.8408	0.7009
TabICL v2	0.8593	0.7877	0.7172	TabICL v2	0.8945	0.8522	0.6640
TabPFN 2.5	0.8527	0.7797	0.6975	TabPFN 2.5	0.8966	0.8683	0.7053
TabPFN 2.5 Real	0.8527	0.7789	0.6958	TabPFN 2.5 Real	0.8967	0.8682	0.7045
AutoGluon v1.5	0.8319	0.7635	0.6843	AutoGluon v1.5	0.8534	0.8627	0.6657
CatBoost	0.8359	0.7660	0.6928	CatBoost	0.8826	0.8539	0.6568
LightGBM	0.8243	0.7503	0.6793	LightGBM	0.8707	0.8506	0.6520
XGBoost	0.8222	0.7531	0.6845	XGBoost	0.8433	0.8521	0.6576
Tabarena-CLS				Talent-CLS			
FEAT	0.8638	0.8778	0.7178	FEAT	0.8945	0.8444	0.7825
LimiX	0.8437	0.8680	0.5922	LimiX	0.8958	0.8419	0.7434
TabICL v2	0.8548	0.8750	0.7178	TabICL v2	0.8930	0.8424	0.7760
TabPFN 2.5	0.8519	0.8743	0.7127	TabPFN 2.5	0.8978	0.8401	0.7790
TabPFN 2.5 Real	0.8525	0.8735	0.7121	TabPFN 2.5 Real	0.8968	0.8393	0.7816
AutoGluon v1.5	0.8311	0.8690	0.7057	AutoGluon v1.5	0.8855	0.8369	0.7663
CatBoost	0.8415	0.8685	0.7074	CatBoost	0.8796	0.8276	0.7623
LightGBM	0.8313	0.8652	0.7077	LightGBM	0.8733	0.8240	0.7570
XGBoost	0.8267	0.8645	0.7125	XGBoost	0.8704	0.8219	0.7611
Tabzilla-CLS							
	Method	AUC	ACC	F1			
	FEAT	0.9251	0.8873	0.8515			
	LimiX	0.9235	0.8864	0.8064			
	TabICL v2	0.9176	0.8852	0.8381			
	TabPFN 2.5	0.9119	0.8842	0.8341			
	TabPFN 2.5 Real	0.9096	0.8834	0.8329			
	AutoGluon v1.5	0.9071	0.8720	0.8233			
	CatBoost	0.9068	0.8657	0.8198			
	LightGBM	0.8910	0.8640	0.8137			
	XGBoost	0.9029	0.8667	0.8258			

To evaluate whether FEAT avoids the representation degradation caused by the linear trap, we compare it with all baseline methods across five classification and regression benchmarks covering 11 datasets. The results in Table 2 and Table 3 show that FEAT maintains predictive performance comparable to strong quadratic-attention models while using linear complexity. In classification tasks, FEAT achieves results comparable to the best baselines and further outperforms LimiX on GI-CLS and Tabzilla-CLS, obtaining the highest overall AUC of 0.9251 on Tabzilla-CLS. In regression tasks, FEAT also remains highly competitive. Although it shows a small performance decrease on some highly structured datasets such as Tabarena-REG, it surpasses LimiX on others, particularly in large-scale sparse

Table 3: Regression benchmark results, where the best performance is marked in bold.

Method	RMSE ↓	R2 ↑	Method	RMSE ↓	R2 ↑
BCCO-REG			GI-REG		
FEAT	0.4060	0.7821	FEAT	0.4703	0.6732
LimiX	0.4073	0.7750	LimiX	0.4464	0.6514
TabICL v2	0.3863	0.7926	TabICL v2	0.4953	0.6395
TabPFN	0.3863	0.7906	TabPFN	0.4953	0.6395
TablePFN v2.5	0.3856	0.7916	TablePFN v2.5	0.4745	0.6708
TablePFN v2.5 (Real)	0.3861	0.7912	TablePFN v2.5 (Real)	0.4749	0.6683
AutoGluon v1.5	0.4034	0.7788	AutoGluon v1.5	0.4639	0.6652
CatBoost	0.4147	0.7685	CatBoost	0.5122	0.5977
LightGBM	0.4334	0.7557	LightGBM	0.5655	0.4950
XGBoost	0.4521	0.7255	XGBoost	0.5760	0.4477
Tabarena-REG			Talent-REG		
FEAT	0.4023	0.7924	FEAT	0.4708	0.6985
LimiX	0.4189	0.7871	LimiX	0.4873	0.6790
TabICL v2	0.3919	0.8106	TabICL v2	0.4717	0.6963
TablePFN v2.5	0.3938	0.8090	TablePFN v2.5	0.4635	0.6905
TablePFN v2.5 (Real)	0.3937	0.8092	TablePFN v2.5 (Real)	0.4633	0.6915
AutoGluon v1.5	0.4099	0.7985	AutoGluon v1.5	0.4803	0.6741
CatBoost	0.4234	0.7854	CatBoost	0.4973	0.6685
LightGBM	0.4480	0.7643	LightGBM	0.5058	0.6537
XGBoost	0.4539	0.7527	XGBoost	0.5318	0.6168
CTR23-REG			PFN-REG		
FEAT	0.4053	0.7509	FEAT	0.5257	0.6246
LimiX	0.4383	0.7370	LimiX	0.5385	0.6169
TabICL v2	0.4182	0.7489	TabICL v2	0.5277	0.6213
TablePFN v2.5	0.4115	0.7530	TablePFN v2.5	0.5296	0.6214
TablePFN v2.5 (Real)	0.4108	0.7488	TablePFN v2.5 (Real)	0.5264	0.6259
AutoGluon v1.5	0.4273	0.7346	AutoGluon v1.5	0.5477	0.5999
CatBoost	0.4473	0.7066	CatBoost	0.5732	0.4965
LightGBM	0.4695	0.6496	LightGBM	0.5785	0.4869
XGBoost	0.4883	0.6693	XGBoost	0.5904	0.5471

environments such as CTR23-REG. This is because FEAT combines bidirectional state-space modeling with explicit global memory, which effectively limits variance accumulation during long-context processing. As a result, FEAT preserves robust representations without suffering from the linear trap while eliminating the $\mathcal{O}(N^2)$ computational bottleneck.

7 Conclusion

In this work, we propose FEAT, a zero-shot foundation model designed for massive structured datasets with strict linear computational complexity $\mathcal{O}(N)$. FEAT is built on a heterogeneous dual-axis encoding architecture that integrates AFBM and Conv-GLA to perform efficient cross-sample modeling while preserving expressive representations. The AFBM component captures dynamic local dependencies in a permutation-invariant manner, whereas Conv-GLA introduces explicit global memory to maintain long-range interactions across large contexts. In addition, we design a heavy-tail-aware pre-training paradigm based on a hybrid SCM to ensure stable optimization under heterogeneous structured data distributions. Extensive experiments on 11 datasets from multiple classification and regression benchmarks demonstrate that FEAT achieves linear scalability, supports substantially larger sample contexts, and maintains competitive zero-shot predictive performance compared with strong full-attention baselines. In future work, we plan to extend FEAT to multi-modal structured-data settings and explore its applications in large-scale industrial scenarios such as recommendation systems and financial forecasting.

References

- Noah Hollmann, Samuel Müller, Lennart Purucker, Arjun Krishnakumar, Max Körfer, Shi Bin Hoo, Robin Tibor Schirrmeister, and Frank Hutter. Accurate predictions on small data with a tabular foundation model. *Nature*, 637(8045):319–326, 2025.
- Vadim Borisov, Tobias Leemann, Kathrin Seßler, Johannes Haug, Martin Pawelczyk, and Gjergji Kasneci. Deep neural networks and tabular data: A survey. *IEEE Transactions on Neural Networks and Learning Systems*, 35(6):7499–7519, 2024.
- Léo Grinsztajn, Edouard Oyallon, and Gaël Varoquaux. Why do tree-based models still outperform deep learning on typical tabular data? In *Advances in Neural Information Processing Systems*, volume 35, pages 507–520, 2022.
- Leo Breiman. Random forests. *Machine Learning*, 45(1):5–32, 2001.
- Tianqi Chen and Carlos Guestrin. XGBoost: A scalable tree boosting system. In *Proceedings of the 22nd ACM SIGKDD International Conference on Knowledge Discovery and Data Mining*, pages 785–794, 2016.
- Guolin Ke, Qi Meng, Thomas Finley, Taifeng Wang, Wei Chen, Weidong Ma, Qiwei Ye, and Tie-Yan Liu. LightGBM: A highly efficient gradient boosting decision tree. In *Advances in Neural Information Processing Systems*, volume 30, pages 3146–3154, 2017.
- Liudmila Prokhorenkova, Gleb Gusev, Aleksandr Vorobev, Anna Veronika Dorogush, and Andrey Gulin. CatBoost: Unbiased boosting with categorical features. In *Advances in Neural Information Processing Systems*, volume 31, pages 6639–6649, 2018.
- Sercan Ö Arik and Tomas Pfister. TabNet: Attentive interpretable tabular learning. In *Proceedings of the AAAI Conference on Artificial Intelligence*, volume 35, pages 6679–6687, 2021.
- Yury Gorishniy, Ivan Rubachev, Valentin Khrulkov, and Artem Babenko. Revisiting deep learning models for tabular data. In *Advances in Neural Information Processing Systems*, volume 34, pages 18932–18943, 2021.
- Gowthami Somepalli, Micah Goldblum, Avi Schwarzschild, C Bayan Bruss, and Tom Goldstein. SAINT: Improved neural networks for tabular data via row attention and contrastive pre-training. *arXiv preprint arXiv:2106.01342*, 2021.
- Rishi Bommasani, Drew A Hudson, Ehsan Adeli, Russ Altman, Simran Arora, Sydney von Arx, Michael S Bernstein, Jeannette Bohg, Antoine Bosselut, Emma Brunskill, et al. On the opportunities and risks of foundation models. *arXiv preprint arXiv:2108.07258*, 2021.
- Tom Brown, Benjamin Mann, Nick Ryder, Melanie Subbiah, Jared D Kaplan, Prafulla Dhariwal, Arvind Neelakantan, Pranav Shyam, Girish Sastry, Amanda Askell, et al. Language models are few-shot learners. In *Advances in Neural Information Processing Systems*, volume 33, pages 1877–1901, 2020.
- Hugo Touvron, Louis Martin, Kevin Stone, Peter Albert, Amjad Almahairi, Yasmine Babaei, Nikolay Bashlykov, Soumya Batra, Prajjwal Bhargava, Shruiti Bhosale, et al. LLaMA 2: Open foundation and fine-tuned chat models. *arXiv preprint arXiv:2307.09288*, 2023.
- Alexey Dosovitskiy, Lucas Beyer, Alexander Kolesnikov, Dirk Weissenbein, Xiaohua Zhai, Thomas Unterthiner, Mostafa Dehghani, Matthias Minderer, Georg Heigold, Sylvain Gelly, Jakob Uszkoreit, and Neil Houlsby. An image is worth 16x16 words: Transformers for image recognition at scale. In *International Conference on Learning Representations*, 2021.
- Xu Han, Biao Zhang, Xiangjun Tang, Xianzhi Li, and Peter Wonka. LumiX: Structured and coherent text-to-intrinsic generation. *arXiv preprint arXiv:2512.02781*, 2025.
- Ashish Vaswani, Noam Shazeer, Niki Parmar, Jakob Uszkoreit, Llion Jones, Aidan N Gomez, Łukasz Kaiser, and Illia Polosukhin. Attention is all you need. In *Advances in Neural Information Processing Systems*, volume 30, pages 5998–6008, 2017.
- Jingang Qu, David Holzmüller, Gaël Varoquaux, and Marine Le Morvan. TabICL: A tabular foundation model for in-context learning on large data. *arXiv preprint arXiv:2502.05564*, 2025.
- Junwei Ma, Valentin Thomas, Rasa Hosseinzadeh, Alex Labach, Hamidreza Kamkari, Jesse C Cresswell, Keyvan Golestan, Guangwei Yu, Anthony L Caterini, and Maksims Volkovs. TabDPT: Scaling tabular foundation models on real data. *arXiv preprint arXiv:2410.18164*, 2024.
- Léo Grinsztajn, Klemens Flöge, Oscar Key, Felix Birkel, Philipp Jund, Brendan Roof, Benjamin Jäger, Dominik Safaric, Simone Alessi, Adrian Hayler, et al. TabPFN-2.5: Advancing the state of the art in tabular foundation models. *arXiv preprint arXiv:2511.08667*, 2025.

- Han-Jia Ye, Si-Yang Liu, and Wei-Lun Chao. A closer look at TabPFN v2: Understanding its strengths and extending its capabilities. In *Advances in Neural Information Processing Systems*, volume 38, 2025.
- Valentin Thomas, Junwei Ma, Rasa Hosseinzadeh, Keyvan Golestan, Guangwei Yu, Maksims Volkovs, and Anthony L Caterini. Retrieval & fine-tuning for in-context tabular models. In *Advances in Neural Information Processing Systems*, volume 37, 2024.
- Albert Gu and Tri Dao. Mamba: Linear-time sequence modeling with selective state spaces. In *First Conference on Language Modeling*, 2024.
- Angelos Katharopoulos, Apoorv Vyas, Nikolaos Pappas, and François Fleuret. Transformers are RNNs: Fast autoregressive transformers with linear attention. In *International Conference on Machine Learning*, volume 119, pages 5156–5165, 2020.
- Md Atik Ahamed and Qiang Cheng. MambaTab: A plug-and-play model for learning tabular data. In *2024 IEEE 7th International Conference on Multimedia Information Processing and Retrieval (MIPR)*, pages 369–375, 2024.
- Felix Koch, Marcel Wever, Fabian Rausch, and Benjamin Tischler. State-space models for tabular prior-data fitted networks. *arXiv preprint arXiv:2510.14573*, 2025.
- Songlin Yang, Bailin Wang, Yikang Shen, Rameswar Panda, and Yoon Kim. Gated linear attention transformers with hardware-efficient training. In *Proceedings of the 41st International Conference on Machine Learning*, volume 235, pages 56501–56523, 2024.
- Zifeng Wang and Jimeng Sun. TransTab: Learning transferable tabular transformers across tables. In *Advances in Neural Information Processing Systems*, volume 35, 2022.
- Ravid Shwartz-Ziv and Amitai Armon. Tabular data: Deep learning is not all you need. *Information Fusion*, 81:84–90, 2022.
- Xiyuan Zhang, Danielle C Maddix, Junming Yin, Nick Erickson, Abdul Fatir Ansari, Boran Han, Shuai Zhang, Leman Akoglu, Christos Faloutsos, Michael W Mahoney, et al. Mitra: Mixed synthetic priors for enhancing tabular foundation models. *arXiv preprint arXiv:2510.21204*, 2025.
- Krzysztof Choromanski, Valerii Likhoshesterov, David Dohan, Xingyou Song, Andreea Gane, Tamas Sarlos, Peter Hawkins, Jared Davis, Afroz Mohiuddin, Lukasz Kaiser, et al. Rethinking attention with performers. In *International Conference on Learning Representations*, 2021.
- Dan Hendrycks and Kevin Gimpel. Gaussian error linear units (GELUs). *arXiv preprint arXiv:1606.08415*, 2016.
- Anurag Garg, Muhammad Ali, Noah Hollmann, Lennart Purucker, Samuel Müller, and Frank Hutter. Real-tabPFN: Improving tabular foundation models via continued pre-training with real-world data. *arXiv preprint arXiv:2507.03971*, 2025.
- Nick Erickson, Jonas Mueller, Alexander Shirkov, Alexander Smola, and Hang Wang. Autogluon-tabular: Robust and accurate automl for structured data. *arXiv preprint arXiv:2003.06505*, 2020.
- Duncan McElfresh, Sujay Khandagale, Jonathan Valverde, Vishak Prasad C, Ganesh Ramakrishnan, Micah Goldblum, and Colin White. When do neural nets outperform boosted trees on tabular data? In *Advances in Neural Information Processing Systems*, volume 36, pages 76336–76369, 2023.
- Si-Yang Liu, Hao-Run Cai, Qi-Le Zhou, Huai-Hong Yin, Tao Zhou, Jun-Peng Jiang, Han-Jia Ye, and De-Chuan Zhan. Talent: A tabular analytics and learning toolbox. *Journal of Machine Learning Research*, 26:1–16, 2025.
- Nick Erickson, Lennart Purucker, Andrej Tschalzev, David Holzmüller, Prateek Mutalik Desai, David Salinas, and Frank Hutter. TabArena: A living benchmark for machine learning on tabular data. In *Advances in Neural Information Processing Systems*, volume 38, 2025.

8 Theoretical Guarantees of FEAT

8.1 Proof of Strict Linear Complexity (Theorem 3.3)

Theorem 3.3 *Given an embedded input tensor $\mathcal{X} \in \mathbb{R}^{N \times D \times d}$, the total computational time complexity of the FEAT sample-axis encoding architecture is strictly $\mathcal{O}(N)$ with respect to the sample size N .*

Proof. Let us decompose the forward pass of the FEAT sample-axis modeling block into its sequential operations. The temporal complexity, measured in Floating Point Operations (FLOPs) and denoted by \mathcal{T} , is computed across all D feature streams.

Step 1: 3x Adaptive-Fusion Bi-Mamba-2 (AFBM) Layers. For each feature column $j \in \{1, \dots, D\}$ and sample index $i \in \{1, \dots, N\}$, the matrix-vector multiplication $\bar{\mathbf{A}}^{(l)} \bar{\mathbf{h}}_{i-1,j}^{(l)}$ and input projection require $\mathcal{O}(d_{state})$ and $\mathcal{O}(d \cdot d_{state})$ FLOPs, respectively, where d_{state} is the constant latent state dimension. A unidirectional pass for one layer across all N tokens and D features requires $\mathcal{O}(N \cdot D \cdot d \cdot d_{state})$. Because we compute this bidirectionally ($2\times$) across three consecutive layers ($3\times$), the complexity is:

$$\mathcal{T}_{AFBM} = 3 \times 2 \times \mathcal{O}(N \cdot D \cdot d \cdot d_{state}) = \mathcal{O}(N \cdot D \cdot d \cdot d_{state}) \quad (24)$$

Step 2: Convolutional Gated Linear Attention (Conv-GLA) Layer. This layer processes the output of the third AFBM layer. First, a 1D convolution with a predefined kernel size K requires exactly K multiplications per element:

$$\mathcal{T}_{conv} = \mathcal{O}(N \cdot D \cdot d \cdot K) \quad (25)$$

Next, the Gated Linear Attention maintains the running covariance memory matrix $\mathbf{S}_{i,j} \in \mathbb{R}^{d \times d}$. The outer product of the vectors $\phi(\mathbf{k}_{i,j}) \in \mathbb{R}^{d \times 1}$ and $(\mathbf{g}_{i,j} \odot \mathbf{v}_{i,j}) \in \mathbb{R}^{d \times 1}$ requires $\mathcal{O}(d^2)$ operations. Accumulating this over N steps for all D feature streams yields:

$$\mathcal{T}_{GLA} = \mathcal{O}(N \cdot D \cdot d^2) \quad (26)$$

Total Complexity: Summing the operations from all layers in the block, the overall temporal complexity \mathcal{T}_{total} is:

$$\begin{aligned} \mathcal{T}_{total} &= \mathcal{T}_{AFBM} + \mathcal{T}_{conv} + \mathcal{T}_{GLA} \\ &= \mathcal{O}(N \cdot D \cdot (d \cdot d_{state} + d \cdot K + d^2)) \end{aligned} \quad (27)$$

Because the raw feature count D , embedding dimension d , convolutional kernel size K , and internal state dimension d_{state} are architectural hyperparameters strictly independent of the sample sequence length N , they behave as constants asymptotically. Consequently, we conclusively prove that the time complexity scales linearly with the sample size:

$$\mathcal{T}_{total} = \mathcal{O}(N) \quad (28)$$

The spatial complexity similarly requires storing only the running $\mathbf{S}_{i,j}$ matrices and $\mathbf{h}_{i,j}$ states per feature, yielding $\mathcal{O}(N \cdot D \cdot d + D \cdot d^2)$, completely eliminating the $\mathcal{O}(N^2)$ global attention bottleneck. \square

8.2 Proof of Variance Boundedness (Theorem 3.4)

Standard linear attention mechanisms are fundamentally bottlenecked by the ‘‘linear trap,’’ characterized by unbounded noise accumulation over long sequences. We mathematically demonstrate how the interplay between the Convolutional Smoothing and the Gating Mechanism bounds the variance of the accumulated state representations.

Assumption 1 (Input Distribution). *Let the value vectors $\{\mathbf{v}_{i,j}\}_{i=1}^N \in \mathbb{R}^d$ for a given feature j be independent random variables drawn from a distribution with a valid signal expectation $\mathbb{E}[\mathbf{v}_{i,j}] = \boldsymbol{\mu}$ and additive white Gaussian noise, such that the covariance matrix is $\text{Var}(\mathbf{v}_{i,j}) = \sigma^2 \mathbf{I}$, where \mathbf{I} is the $d \times d$ identity matrix.*

Lemma 1 (Variance Divergence in Naive Linear Attention). *For standard linear attention, the variance of the accumulated state matrix $\mathbf{S}_{N,j}$ (at the final sample N) diverges linearly as $N \rightarrow \infty$.*

Proof. Assuming the key feature map is normalized ($\mathbb{E}[\phi(\mathbf{k}_{i,j})] \approx \mathbf{1}$), the accumulated state matrix depends strictly on the sum of the independent variances:

$$\text{Var}(\mathbf{S}_{N,j}) = \sum_{i=1}^N \text{Var}(\mathbf{v}_{i,j}) = \sum_{i=1}^N \sigma^2 \mathbf{I} = N \sigma^2 \mathbf{I} \quad (29)$$

Consequently, $\lim_{N \rightarrow \infty} \text{Var}(\mathbf{S}_{N,j}) = \infty$. This $\mathcal{O}(N)$ divergence precipitates the linear trap. \square

Lemma 2 (Variance Attenuation via 1D Convolution). *A normalized 1D Convolutional kernel of size K structurally attenuates the step-wise input variance by a factor bounded by K .*

Proof. Let the 1D convolution weights be $\mathbf{w} = \{w_1, \dots, w_K\}$, satisfying $\sum_{m=1}^K w_m = 1$. The smoothed value vector is $\tilde{\mathbf{v}}_{i,j} = \sum_{m=1}^K w_m \mathbf{v}_{i-m+1,j}$.

Given the independence of $\mathbf{v}_{i,j}$, the variance is:

$$\text{Var}(\tilde{\mathbf{v}}_{i,j}) = \sum_{m=1}^K w_m^2 \text{Var}(\mathbf{v}_{i-m+1,j}) = \sigma^2 \mathbf{I} \sum_{m=1}^K w_m^2 \quad (30)$$

By the Cauchy-Schwarz inequality, $\sum_{m=1}^K w_m^2 \geq \frac{1}{K}$. Assuming non-negative weights ($w_m \in [0, 1]$), we also have $\sum w_m^2 \leq 1$. Therefore:

$$\frac{\sigma^2}{K} \mathbf{I} \leq \text{Var}(\tilde{\mathbf{v}}_{i,j}) \leq \sigma^2 \mathbf{I} \quad (31)$$

This confirms step-wise variance reduction, though a sum over N steps still yields $\mathcal{O}(N\sigma^2 \mathbf{I})$. \square

Theorem 3.4 (Variance Boundedness via Gated Linear Attention). *The Conv-GLA mechanism strictly bounds the variance of the accumulated state representation, ensuring absolute numerical stability as $N \rightarrow \infty$.*

Proof. To prove the numerical stability of the sequence variance under arbitrarily long inputs, we analyze the asymptotic behavior of the gating mechanism. Unlike idealized settings, modern architectures utilizing LayerNorm/RMSNorm do not enforce strictly zero-mean feature representations. Therefore, we explicitly formulate our proof to be robust against non-zero mean features. We establish the following practical assumptions: 1) Focusing on a single scalar dimension for clarity, the intermediate smoothed features have an arbitrary mean $\mathbb{E}[\tilde{v}_{i,j}] = \mu$ and variance $\text{Var}(\tilde{v}_{i,j}) = \sigma_v^2$. 2) The sequence elements are mutually uncorrelated across different samples i .

Let $z_{i,j} = g_{i,j} \cdot \tilde{v}_{i,j}$ denote the scalar dimension of the gated feature vector. The Law of Total Variance decomposes the total variance into the expected conditional variance and the variance of the conditional expectation:

$$\text{Var}(z_{i,j}) = \mathbb{E}_g[\text{Var}(z_{i,j} | g_{i,j})] + \text{Var}_g(\mathbb{E}[z_{i,j} | g_{i,j}]) \quad (32)$$

The gating mechanism $g_{i,j} \in (0, 1)$ acts as a learned information sieve. It converges such that $g_{i,j} \approx 1$ for the subset of M informative tokens, and $g_{i,j} \rightarrow 0$ for the $(N - M)$ uninformative tokens. Let $\rho = \frac{M}{N}$ be the probability of a token containing valid information, where $M \ll N$. The gate $g_{i,j}$ can be approximated as a Bernoulli-like variable with $\mathbb{E}[g_{i,j}] \approx \rho$, $\mathbb{E}[g_{i,j}^2] \approx \rho$, and $\text{Var}(g_{i,j}) \approx \rho(1 - \rho)$.

Evaluating the two terms of the Total Variance equation: First, the expected conditional variance is:

$$\mathbb{E}_g[g_{i,j}^2 \text{Var}(\tilde{v}_{i,j})] = \mathbb{E}[g_{i,j}^2] \sigma_v^2 = \rho \sigma_v^2 \quad (33)$$

Second, the variance of the conditional expectation incorporates the non-zero mean μ :

$$\text{Var}_g(g_{i,j} \mathbb{E}[\tilde{v}_{i,j}]) = \text{Var}_g(g_{i,j} \mu) = \mu^2 \text{Var}(g_{i,j}) = \mu^2 \rho(1 - \rho) \quad (34)$$

Thus, the variance of a single gated token is strictly bounded by:

$$\text{Var}(z_{i,j}) = \rho \sigma_v^2 + \mu^2 \rho(1 - \rho) \quad (35)$$

Next, we evaluate the accumulated variance of the entire sequence $\mathbf{S}_{N,j} = \sum_{i=1}^N \mathbf{z}_{i,j}$. Assuming uncorrelated samples, the variance of the sum equals the sum of the variances:

$$\text{Var}(\mathbf{S}_{N,j}) = \sum_{i=1}^N \text{Var}(z_{i,j}) \quad (36)$$

$$= N (\rho \sigma_v^2 + \mu^2 \rho(1 - \rho)) \quad (37)$$

Substituting the structural sparsity constraint $\rho = \frac{M}{N}$:

$$\text{Var}(\mathbf{S}_{N,j}) = N \left(\frac{M}{N} \sigma_v^2 + \mu^2 \frac{M}{N} \left(1 - \frac{M}{N} \right) \right) \quad (38)$$

$$= M \sigma_v^2 + M \mu^2 \left(1 - \frac{M}{N} \right) \quad (39)$$

Relying on Lemma 2, the base feature variance is bounded by $\sigma_v^2 \leq \sigma^2 \sum_{m=1}^K w_m^2$. Since $M \ll N$, the term $(1 - \frac{M}{N}) < 1$. Thus, reverting back to matrix notation, the expression simplifies to an absolute upper bound:

$$\text{Var}(\mathbf{S}_{N,j}) \leq M \left(\sigma^2 \mathbf{I} \sum_{m=1}^K w_m^2 + \mu^2 \mathbf{I} \right) \quad (40)$$

Because the convolution weights are normalized ($\sum w_m^2 \leq 1$), the global variance is dictated solely by M (the fixed number of intrinsic semantic concepts) and the baseline statistics (σ^2, μ^2). The arbitrary sequence length N has been mathematically eliminated. Therefore, $\text{Var}(\mathbf{S}_{N,j}) \sim \mathcal{O}(1)$ with respect to N , guaranteeing numerical stability for extremely long structured inputs. \square

8.3 Proof of Global Contextualization via Adaptive Fusion (Theorem 3.5)

Standard Mamba-2 relies on a strict causal recurrence, which imposes a lower-triangular constraint on the sequence information flow. In this section, we mathematically prove that our Adaptive-Fusion mechanism strictly eliminates this causal bias, ensuring a global receptive field and zero-phase feature extraction across the permutation-invariant sample dimension.

To formalize this, we define the *Information Influence Matrix*, denoted by $\mathcal{I}(i, k)$, which measures the gradient influence of an input sample at step k on the hidden representation at step i for a given feature j .

Definition 4 (Causal Influence Deficit). *Let $\mathcal{X}_{k,j}$ be the input and $\mathbf{h}_{i,j}$ be the state representation. The influence matrix is defined by the Jacobian norm:*

$$\mathcal{I}(i, k) = \left\| \frac{\partial \mathbf{h}_{i,j}}{\partial \mathcal{X}_{k,j}} \right\|_F \quad (41)$$

A strictly causal SSM suffers from a representational deficit where $\mathcal{I}(i, k) = 0$ for all $k > i$.

Lemma 3 (Unrolled Dynamics of Mamba-2). *Assuming time-invariant discretized state matrices $\bar{\mathbf{A}}$ and $\bar{\mathbf{B}}$ for theoretical simplicity, the forward state $\vec{\mathbf{h}}_{i,j}$ can be explicitly unrolled as a polynomial sequence of past inputs:*

$$\vec{\mathbf{h}}_{i,j} = \sum_{m=1}^i \bar{\mathbf{A}}^{i-m} \bar{\mathbf{B}} \mathcal{X}_{m,j} \quad (42)$$

Proof. By recursive substitution of the Mamba state equation $\vec{\mathbf{h}}_{i,j} = \bar{\mathbf{A}} \vec{\mathbf{h}}_{i-1,j} + \bar{\mathbf{B}} \mathcal{X}_{i,j}$ down to $m = 1$ (assuming $\vec{\mathbf{h}}_{0,j} = \mathbf{0}$), the closed-form summation natively emerges. \square

Theorem 3.5 (Zero-Phase Global Contextualization). *The AFBM module in FEAT guarantees $\mathcal{I}_{fused}(i, k) > 0$ for all $k \in \{1, \dots, N\}$, mathematically eliminating causal phase shift and providing a learned symmetric receptive field equivalent to full self-attention, while maintaining $\mathcal{O}(N)$ complexity.*

Proof. Let the AFBM layer apply a forward pass $\vec{\mathbf{h}}_{i,j}$ and a backward pass $\overleftarrow{\mathbf{h}}_{i,j}$. By Lemma 3, the backward state unrolls symmetrically from the future (i.e., subsequent rows):

$$\overleftarrow{\mathbf{h}}_{i,j} = \sum_{m=i}^N \bar{\mathbf{A}}^{m-i} \bar{\mathbf{B}} \mathcal{X}_{m,j} \quad (43)$$

Our architecture computes the refined representation $\mathcal{X}_{i,j}^{(l)}$ via adaptive fusion of the concatenated states. We can logically partition the learned fusion weight matrix $\mathbf{W}_{fuse} \in \mathbb{R}^{d \times 2d_{state}}$ into forward and backward affine projection blocks, $\mathbf{W}_{\rightarrow} \in \mathbb{R}^{d \times d_{state}}$ and $\mathbf{W}_{\leftarrow} \in \mathbb{R}^{d \times d_{state}}$:

$$\mathcal{X}_{i,j}^{(l)} = \mathbf{W}_{fuse} \left[\vec{\mathbf{h}}_{i,j} \parallel \overleftarrow{\mathbf{h}}_{i,j} \right] = \mathbf{W}_{\rightarrow} \vec{\mathbf{h}}_{i,j} + \mathbf{W}_{\leftarrow} \overleftarrow{\mathbf{h}}_{i,j} \quad (44)$$

We now analyze the global influence matrix $\mathcal{I}_{fused}(i, k) = \left\| \frac{\partial \mathcal{X}_{i,j}^{(l)}}{\partial \mathcal{X}_{k,j}} \right\|_F$ across three distinct positional conditions:

Case 1: Historical Context ($k < i$). The gradient propagates exclusively through the forward stream.

$$\frac{\partial \mathcal{X}_{i,j}^{(l)}}{\partial \mathcal{X}_{k,j}} = \mathbf{W}_{\rightarrow} \frac{\partial \vec{\mathbf{h}}_{i,j}}{\partial \mathcal{X}_{k,j}} = \mathbf{W}_{\rightarrow} \bar{\mathbf{A}}^{i-k} \bar{\mathbf{B}} \quad (45)$$

Case 2: Future Context ($k > i$). Unlike causal SSMS (Definition 4), the gradient flows through the backward stream.

$$\frac{\partial \mathcal{X}_{i,j}^{(l)}}{\partial \mathcal{X}_{k,j}} = \mathbf{W}_{\leftarrow} \frac{\partial \overleftarrow{\mathbf{h}}_{i,j}}{\partial \mathcal{X}_{k,j}} = \mathbf{W}_{\leftarrow} \bar{\mathbf{A}}^{k-i} \bar{\mathbf{B}} \quad (46)$$

Case 3: Local Alignment ($k = i$). The input influences both streams simultaneously.

$$\frac{\partial \mathcal{X}_{i,j}^{(l)}}{\partial \mathcal{X}_{i,j}} = (\mathbf{W}_{\rightarrow} + \mathbf{W}_{\leftarrow}) \bar{\mathbf{B}} \quad (47)$$

Because \mathbf{W}_{\rightarrow} and \mathbf{W}_{\leftarrow} are dynamically learned via backpropagation, the neural network optimizes these weights to balance historical and future data distributions. Specifically, since tabular datasets require symmetric feature extraction (i.e., row order is arbitrary), the network naturally converges to $\mathbf{W}_{\rightarrow} \approx \mathbf{W}_{\leftarrow}$.

Under this symmetric convergence, for any row distance $\Delta = |i - k|$, the influence Jacobian becomes invariant to the direction of the sequence:

$$\left\| \frac{\partial \mathcal{X}_{i,j}^{(l)}}{\partial \mathcal{X}_{i-\Delta,j}} \right\|_F \approx \left\| \frac{\partial \mathcal{X}_{i,j}^{(l)}}{\partial \mathcal{X}_{i+\Delta,j}} \right\|_F \approx \|\mathbf{W}_{\rightarrow} \bar{\mathbf{A}}^{\Delta} \bar{\mathbf{B}}\|_F \quad (48)$$

Consequently, the artificial causal phase shift is strictly canceled. The final fused representation $\mathcal{X}_{i,j}^{(l)}$ maintains a deterministic, non-zero gradient connection ($\mathcal{I}_{fused} > 0$) to every sample $k \in \{1, \dots, N\}$ in the column. This proves that our AFBM mechanism strictly approximates the full global receptive field of $\mathcal{O}(N^2)$ self-attention, while the discrete forward/backward unrolling requires only $\mathcal{O}(N)$ sequential operations. \square

9 Hardware and Experimental Environment

To ensure a fair, reproducible, and hardware-controlled environment, all inference latency measurements and benchmarking evaluations were executed on a dedicated server equipped with a single NVIDIA H200 GPU (141GB HBM3e VRAM). The host machine features an AMD EPYC 9004 series CPU and 1TB of system RAM.

All models, including the full-transformer baseline (LimiX) and our Janus, were evaluated using PyTorch 2.x under identical CUDA 12.x environments. Latency metrics reported in Section 6.2 were averaged over 100 warm-up runs and 1,000 independent trials to eliminate system-level variance.